applied optics

Fabrication of a high-accuracy phase-type computer-generated hologram by physical vapor deposition

Zhiyu Zhang,[1,*] Ruoqiu Wang,[1] Teng Hao,[2] Chengli Guo,[2] Donglin Xue,[1] and Xuejun Zhang[1]

[1]Key Laboratory of Optical System Advanced Manufacturing Technology, Changchun Institute of Optics, Fine Mechanics and Physics, Chinese Academy of Sciences, Changchun, Jilin 130033, China
[2]University of Chinese Academy of Sciences, Beijing 100049, China
*Corresponding author: zhangzhiyu@ciomp.ac.cn

Received 3 July 2018; revised 23 August 2018; accepted 23 August 2018; posted 23 August 2018 (Doc. ID 337593); published 20 September 2018

With the development of optical systems used in astronomical and earth observation, aspherical and free-form surfaces are increasingly used because they are lightweight and have improved image quality. As a highly accurate, aberrationless technique, computer-generated hologram (CGH) plays an important role in wavefront testing. At present, the main way to fabricate phase CGH is reactive ion etching, which suffers from low accuracy. To improve the accuracy, physical vapor deposition (PVD) is applied in the fabrication of phase CGH. The wavefront errors of PVD-fabricated phase CGH were analyzed. Testing results indicate that the wavefront error of the CGH is 0.020λ root mean square (RMS), mainly caused by the machine tool orthogonality error rather than the PVD process. The diffraction efficiency of the +1st order is 22.4%.

https://doi.org/10.1364/AO.57.000F31

1. INTRODUCTION

Testing of a spherical mirror surface is typically performed using an interferometer. During measurement, the surface being tested is illuminated with a coherent spherical wave, and deviations of the surface shape from this wave could be characterized to nanometer order accuracy [1,2]. In recent years, aspherical optics and free forms have been widely used in optical systems to provide improved imaging performance as well as offering a reduced size and weight. However, an interferometer cannot be used directly to measure aspherical surfaces. A compensator must be used to change the spherical wavefront to aspherical one before an interferometer is used in aspherical testing, similar to the testing of a general sphere.

Computer-generated hologram (CGH) is an effective element to compensate wavefront. The high degree of flexibility in generating complex wavefronts has made CGHs extremely useful compared to conventional null-lens compensators. Thus, these CGHs represent a ruler for the aspherical surface. To some extent, the measurement results depend on the accuracy of the CGHs. Therefore, the CGHs must be accurately fabricated.

A CGH typically consists of a binary circular grating, of either amplitude or phase type, with a locally varying period [3]. CGHs are usually fabricated by photolithography followed by reactive ion etching (RIE). The fabrication errors can be categorized as horizontal errors (including pattern distortion and linewidth deviation) and vertical errors (including etching depth errors and surface roughness). The horizontal errors are related to the accuracy of the pattern generation machine such as laser direct writing or electron beam matching. Vertical errors are mainly affected by the post-fabrication process, especially the etching process. The depth uniformity of an etched surface, for example, is one of the most important evaluating indicators for CGHs. It is usually determined by the related ion energy distribution.

RIE was originally developed to make semiconductor devices [4]. The depth inhomogeneity achieved by commercial RIE equipment for a sample with a diameter up to 200 mm is typically larger than 5%, which is not accurate enough for CGH. To improve depth uniformity, Wang [5] investigated a Teflon annular disk that is used to enclose the substrate in the RIE process. By employing these improvements, a CGH with a 50 mm diameter was made with only a 2% variation in the etching depth uniformity. Wang [6] also proposed a dielectric layer method, in which a thin dielectric layer was first coated on substrate and then a thick layer of SiO_2 was deposited. Because the dielectric coating has very low etch rate for RIE, it acts as a stop layer for the etching process. With this process, very good pattern height uniformity, limited only by the coating uniformity, can be achieved. However, the dielectric layer affects the CGH performance.

Until now, because there has been few effective ways to achieve high-precision phase-type CGH, the amplitude-type

CGH, also called the chrome-on-glass type, is used as an alternative. However, amplitude-type CGH has several shortcomings, which include a lower diffractive efficiency and an indistinguishable zero order of diffraction [7–9].

In the micro/nano machining field, two machining methods are popular. One is a top-down by reducing material; the other is a bottom-up by additive manufacturing [10]. Although the etching technologies were used to meet general requirements, the depth uniformity of groove structures is not well satisfied. On the other hand, the additive method is being applied to obtain a high-precision pattern. However, to the best of our knowledge, there are few reports on the fabrication of CGH. It is required that the coated layer has the same performances (refractive index, uniformity, purity, stress) with those of the substrate, inducing no influence on the testing performances of CGH.

In the present work, an additive method was proposed to fabricate high-precision CGH. By means of physical vapor deposition (PVD), a thin layer of SiO_2 was coated on the predeveloped photoresist mask on fused silica substrate. The performance of the fabricated CGH was evaluated. It is expected that the PVD method could be an effective way to achieve high-precision phase-type CGHs.

2. EXPERIMENT

A. Fabrication Procedure

The fabrication process for phase-type CGH by PVD is shown in Fig. 1. First, a layer of photoresist (AZ4562) with a thickness of 1 μm was spin-coated on fused silica substrate. Then, a DWL4000 laser scanning lithography system (Heidelberg Instruments Mikrotechnik GmbH, Germany) was used to generate the diffraction microstructures. Then, a layer of SiO_2 was deposited by PVD. The equipment used in the present work was a TRP-450 three-target fully automatic magnetron coating system (SKY Technology Development Co., Ltd., CAS, Shenyang, China, formerly known as Shenyang Scientific Instrument R&D Center CAS). The system was a non-equilibrium magnetron sputtering device. Finally, the photoresist was removed. Experimental parameters are given in Tables 1 and 2.

B. Linewidth Calibration

Linewidth deviation is one of the main errors for CGH. To investigate the most suitable conditions for linewidth, four groups of comparison experiments (A, B, C, and D) were performed. The parameters for the process are shown in Table 3. After development, impurities such as residual photoresist were removed using an oxygen ion. The equipment used for

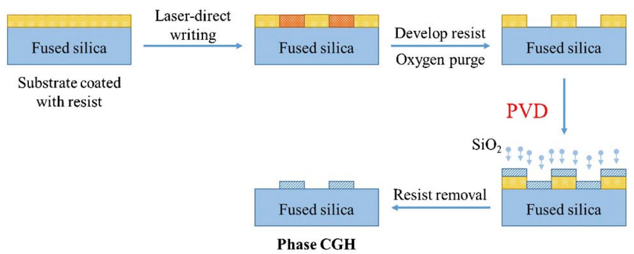

Fig. 1. Fabrication process of phase-type CGH by PVD.

Table 1. Fabrication Parameters for Phase CGH

Items	Parameters
Laser energy/mW	105
Laser focus/mm	30
CD bias/nm	−100
Photoresist thickness/μm	1.1
Development time/s	100
Oxygen purge/s	20

Table 2. Parameters for Magnetron Sputtering Deposition

Items	Parameters
Target source model	High purity silicon oxide
Deposition time/min	60
Sputtering power/W	150
Vacuum degree/Pa	4.0×10^{-4}
Gas flow/sccm	Ar: 80, O_2: 10
Air pressure/Pa	0.87
Temperature/°C	30
Rotation speed/(r/min)	150

Table 3. Parameters for Pretreatment Processes

Items	Hard Bake	Oxygen Purge	Remove Method of Photoresist
A	Yes	30 s	Soaking removal
B	Yes	No	Soaking removal
C	Yes	30 s	Acetone ultrasonic
D	No	30 s	Soaking removal

the oxygen cleaning was a Phantom III RIE machine (Trion Technology, Clearwater, FL, USA). In general, the rate of oxygen cleaning is about 1–2 nm/s, which does not cause obvious damage to the photoresist structure.

After different pretreatments, the four group samples were deposited by SiO_2 using magnetron sputtering. The thickness of the deposition layer was 300 nm. After the removal of the photoresist mask, the surface was observed and measured by a laser confocal microscope.

C. Diffraction Efficiency Testing

When testing CGH, in addition to accuracy, it is necessary to have sufficient diffraction efficiency to identify the bright and dark fringes. To test diffraction efficiency, as shown in Fig. 2, a semiconductor laser ($\lambda = 640$ nm) was used to irradiate the CGH, and a Thorlabs PM201 optical power meter (Thorlabs Inc., Newton, NJ, USA) was used to measure the diffraction efficiency. At the same time, the light powers of the background light, the ejection light, the −1, 0, and +1 orders also were measured.

D. Fabrication Accuracy Evaluation

To realize high-precision testing, the wavefront error of the CGH must be small enough to improve the degree of certainty in the test results. The evaluation of CGH accuracy is very

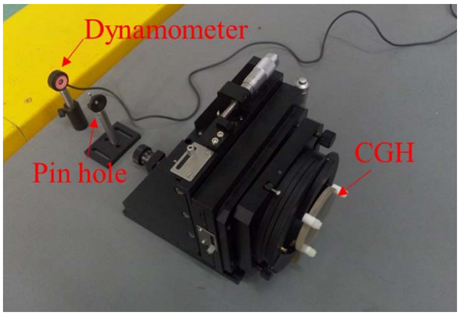

Fig. 2. Testing setups for diffraction efficiency.

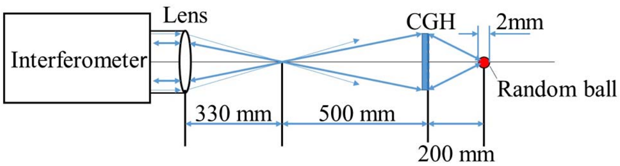

Fig. 3. Schematic of optical setup for accuracy evaluation.

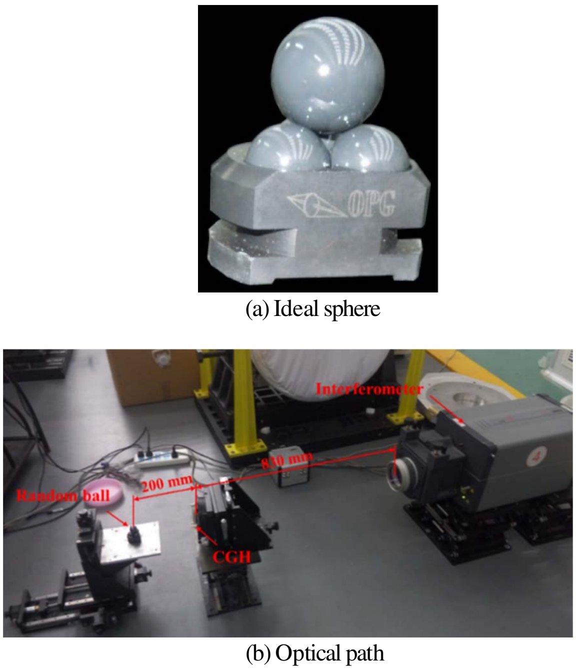

Fig. 4. Evaluation method for CGH accuracy.

important, but has not been widely reported. In this paper, an ideal sphere measurement, as shown in Figs. 3 and 4, was proposed. Measurement parameters are given in Table 4. A ceramic ball with extremely high precision (RMS = $\lambda/1000$, negligible error) is used as a standard target to be measured [11]. During the measurement, the focal point of the first-order diffraction light converges to the center of the sphere, reflects on the surface of the ceramic ball, and then transfers into the interferometer through the CGH.

Table 4. Parameters for Accuracy Evaluation

Items	Parameters
Wavelength/λ	632.8 nm
Reference sphere/F#	3.3
Focal length of Reference sphere/f	330
RMS value	$\lambda/100$
Effective diameter of the CGH	50 mm
Focal length of CGH/f_{cgh}	1000/7 mm
Diameter of the ideal ball	20 mm
Precision of the ideal ball	$\lambda/1000$

3. RESULTS

A. Surface Quality

The variation of the surface roughness causes different amounts of the scattered loss, which leads to wavefront errors. The local variation in surface roughness could also induce the deviation of actual depth. Therefore, the surface roughness must first be controlled.

To verify the surface quality of the PVD layer, the substrate surface was measured before and after magnetron sputtering by an interferometer (Zygo Corp., Middlefield, CT, USA). The results are shown in Fig. 5. It can be seen from the images that the PV value of the substrate is larger after the PVD. Moreover, the low frequency error, such as the four-order Zernike error of the substrate material, was compensated after the growth of the SiO_2 layer. Therefore, the surface shape is better than the surface of the substrate before PVD. In addition, the results also show that the stress deformation caused by SiO_2 and the substrate expansion coefficient is negligible.

The surface roughness was measured using a Zygo white light interferometer. In Fig. 6, there is little difference for the mean Ra value between the deposited layer and the substrate. The PV value is much larger, which may be caused by dust pollution before the growth of the substrate. In addition, the average value of its PV is about 10 nm, which was obtained by averaging the PV values in different small regions.

B. Linewidth Correction

Figure 7(a) shows the patterns on the photoresist mask, while Fig. 7(b) shows the patterns before the removal of the photoresist. Figures 7(c)–7(f) are the results for the comparison mentioned above in Table 3. In Fig. 7(c), the line edge was clear and there was no obvious stripping phenomenon. In Figs. 7(d) and 7(e), the lines have irregular edges and a large number of structures are peeling off. In Fig. 7(f), there was a large amount of suspension after ultrasonic cleaning. As a result, the most suitable parameters for the experimental conditions are found in Fig. 7(c), namely Group A.

For Group A, the linewidths were measured before and after the photoresist removal. Figure 8 shows the data for each linewidth. It can be seen that the linewidth at the bottom of groove is about 0.25 μm narrower than the designed linewidth. However, after the magnetron sputtering deposition, linewidth of the groove is 0.65 μm narrower than the designed linewidth. When the photoresist removed, the linewidth is 0.1 μm wider than the designed linewidth. The final measured linewidth is 0.75 μm wider than that after development on the photoresist. Based on the above result, it can be concluded that

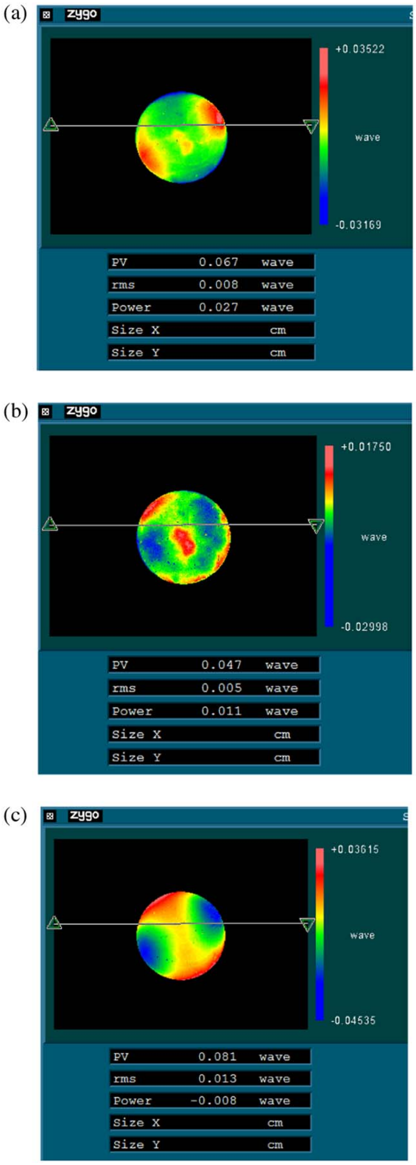

Fig. 5. Surface profiles: (a) Before PVD, (b) PVD surface, and (c) deviation.

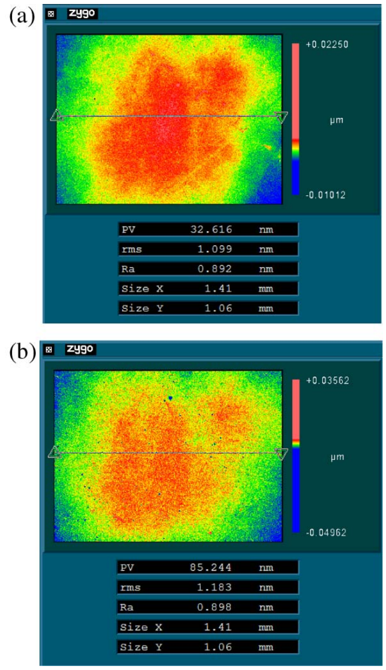

Fig. 6. Surface roughness: (a) Before PVD and (b) PVD surface.

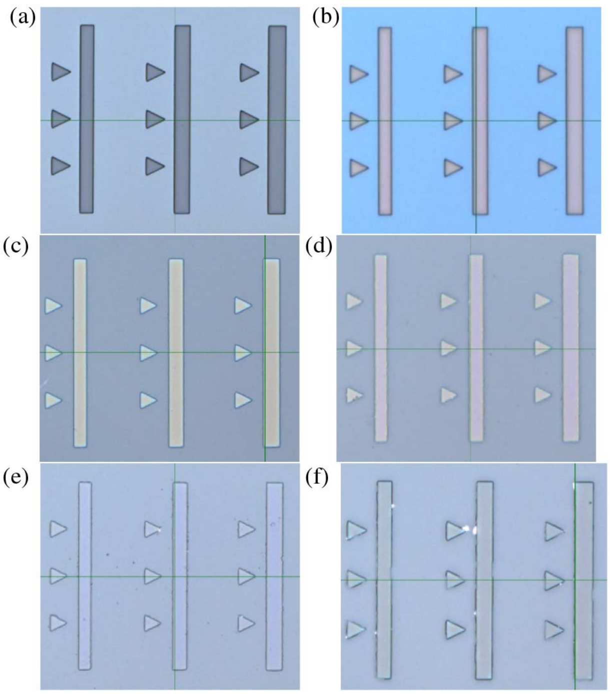

Fig. 7. Images with linewidths of 7, 8, and 9 μm: (a) On photoresist mask, (b) before removal of photoresist, and (c)–(f) after removal of photoresist, corresponding to the pretreatments in Table 3, respectively.

the deposition of magnetron sputtering will result in an increase in the linewidth.

As shown in Fig. 9, in the process of magnetron sputtering, both the photoresist surface and the grooves' bottom were deposited by the SiO_2 layer. During the photoresist removal, the fracture position of the SiO_2 layer should be the weakest region, in the middle of the side wall, not at the top nor the bottom. Therefore, the linewidth was widened to a certain extent. At the same time, due to the poor edge of the groove and the bottom line, the thinnest position of the side wall was varying, which lead to the irregular edge.

There are two ways to deal with the problem of a broadening linewidth. One option is to set appropriate reduction coefficients for the linewidth. This method can only adjust the linewidth. It cannot deal with the irregular edge peeling off. The other option is to use a negative photoresist during photolithography.

C. Observation of Phase-Type CGH

The obtained phase-type CGH is shown in Fig. 10. The main region is 50 mm in diameter with changing linewidths from 160 to 1.6 μm. Figure 11 shows the local topography of the

CGH. It can be seen that the profile of the grooves were clearly fabricated. The minimum width of the groove is 1.6 μm with a sidewall angle of about 70 deg. Results show that the duty ratio is close to 50% and the mean depth is 300 nm with a 1% depth uniformity.

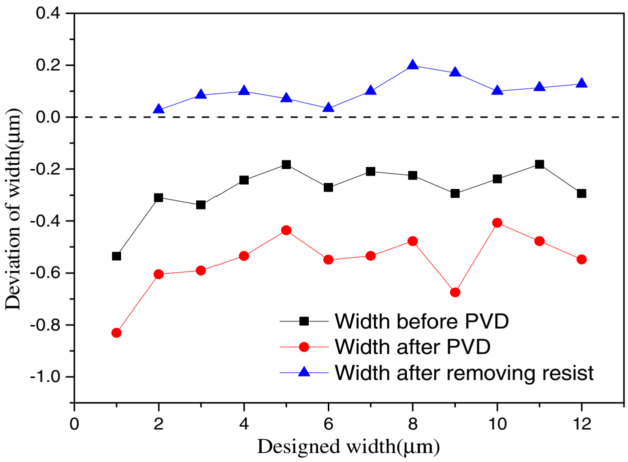

Fig. 8. Deviations of linewidth under different conditions.

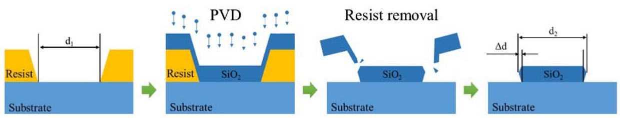

Fig. 9. Schematic diagram of fracture in SiO_2 layer.

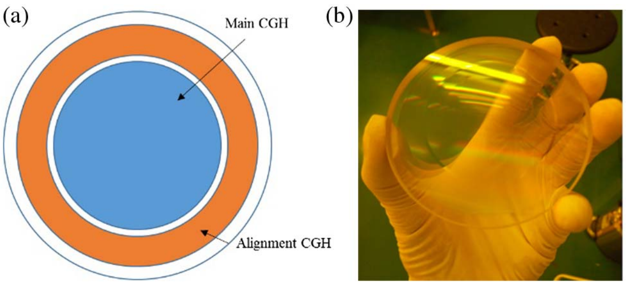

Fig. 10. Fabricated CGH by PVD: (a) Functional areas of the CGH and (b) photo of the fabricated CGH.

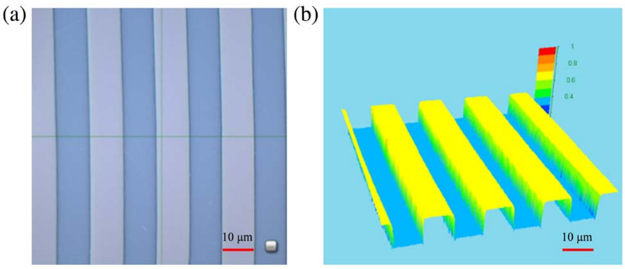

Fig. 11. Local topography of the CGH: (a) Two-dimensional view and (b) three-dimensional profile.

D. Diffraction Efficiency

Figure 12 shows the distribution of diffraction orders. Table 5 shows the measured power of diffraction light. Under the conditions of the present work, the theoretical diffraction efficiency (either −1 or +1 order) is 24.1%. Measured results show that the diffraction efficiency of −1 and +1 is 21.4% and 22.4%, reaching 88.7% and 92.9% of the ideal diffraction efficiency, respectively. The results show that the PVD process has a similar energy loss compared to the traditional etching method. The energy loss may be caused by the absorption of substrate materials, the reflection, and the scattering of the substrate surfaces.

E. CGH Accuracy

The testing results for the fabricated CGH is shown in Fig. 13. The results show that the measured accuracy was 0.02λ RMS (approximate to 12 nm, $\lambda = 632.8$ nm), indicating that the fabrication error is small and the fabricated CGH could meet the measurement requirement.

To analyze the error generation, the first nine Zernike coefficients in Fig. 13 were extracted and shown in Table 6. It is found that the tilt, defocus, and astigmatism are the main errors. Because the tilt and defocus have been filtered in the interferometer measurement, the astigmatism was the main

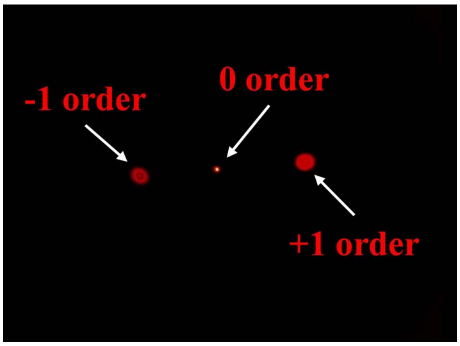

Fig. 12. Distribution of diffraction orders.

Table 5. Power of Diffraction Light

	Background Light	Emission Light	−1 order	0 order	+1 order
Power (μW)	0.009	8.770	1.881	2.541	1.968

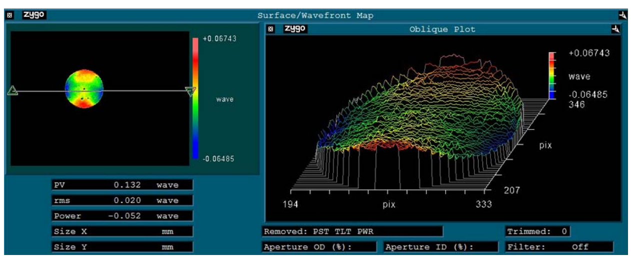

Fig. 13. Wavefront error of the fabricated CGH.

Table 6. Zernike Coefficients in Fig. 12

1	2	3	4	5	6	7	8	9
Alignment region								
0.245	0.173	−0.070	0.015	−0.039	0.017	−0.001	0.002	−0.011
Main region								
0.477	−0.093	0.426	−0.026	−0.045	0.009	0.004	0.000	0.003

factor affecting CGH accuracy. In our previous work, the error of machine tool orthogonality will lead to Zernike astigmatism in CGH measurement [11]. Therefore, it is assumed that the astigmatic error was mainly caused by machine tool orthogonality. In our next paper, the orthogonality issue will be discussed and resolved. A CGH with even higher accuracy could be expected.

In this work, the most significant benefit of PVD-fabricated CGH was improved depth uniformity. The superiority of coating compared with etching was also reflected in the control of the linewidth. A CGH with a much narrower line, which means a larger wavefront slope, could be precisely fabricated by the PVD process. It was also shown that PVD could obtain a steeper sidewall than what etching could. In addition, it is known that the coating process is much cheaper than etching. Therefore, PVD-fabricated CGH has a much lower cost. As a result, we think that the PVD process has great potential in the fabrication of CGHs applied in aspherical/free-form testing and even multiple CGHs in one substrate.

4. CONCLUSIONS

In this work, the combined use of laser lithography and PVD was applied to fabricate CGH. A phase CGH with a minimum linewidth of 1.6 μm was fabricated on the 80 mm × 8 mm fused silica substrate. The test results show that the RMS value of the main region is $\lambda/50$, and the first-order diffraction efficiency is 22.4%. The result shows that the phase CGH produced by PVD has high precision and diffraction efficiency. Considering the influence of the orthogonality error of the laser direct writing machine, the precision of phase-type CGH based on PVD can still be further improved.

This research work provides a cost-effective method to fabricate high-performance optical components. The achievements obtained in the work could also be used in visible and infrared optical applications such as a cellphone camera, a flat panel display, and for night driving assistance, as well as in a next-generation space telescope.

Funding. National Natural Science Foundation of China (NSFC) (51305422, 51775531, 61605202); National 973 Program of China (2014AA014402); Youth Innovation Promotion Association of the Chinese Academy of Sciences (CAS) (2014197).

Acknowledgment. We thank Professor Cunzhu Tong at the State Key Laboratory of Luminescence and Applications, Changchun Institute of Optics, Fine Mechanics and Physics, Chinese Academy of Sciences for the use of their RIE equipment.

REFERENCES

1. J. Ni, C. Wang, C. Zhang, Y. Hu, L. Yang, Z. Lao, B. Xu, J. Li, D. Wu, and J. Chu, "Three-dimensional chiral microstructures fabricated by structured optical vortices in isotropic material," Light Sci. Appl. **6**, e17011 (2017).
2. R. Wang, Z. Zhang, C. Guo, D. Xue, and X. Zhang, "Effects of fabrication errors on diffraction efficiency for a diffractive membrane," Chin. Opt. Lett. **14**, 120501 (2016).
3. C. Guo, Z. Zhang, D. Xue, L. Li, R. Wang, X. Zhou, F. Zhang, and X. Zhang, "High-performance etching of multilevel phase-type Fresnel zone plates with large apertures," Opt. Commun. **407**, 227–233 (2018).
4. Z. Zhang, C. Guo, R. Wang, H. Hu, X. Zhou, T. Liu, D. Xue, X. Zhang, F. Zhang, and X. Zhang, "Hybrid-level Fresnel zone plate for diffraction efficiency enhancement," Opt. Express **25**, 33676–33687 (2017).
5. Q. Wang, L. Chen, and U. Griesmann, *A Simple Method to Improve Etching Uniformity When Making Phase Type CGHs on a Thick Glass Substrate, Optical Fabrication & Testing, Technical Digest (CD)* (Optical Society of America, 2010), p. OWA2.
6. Q. Wang, G. Gao, and U. Griesmann, "Radius measurement of spherical surfaces with large radii-of-curvature using dual-focus zone plates," in *Optical Fabrication and Testing, Technical Digest (CD)* (Optical Society of America, 2008), pp. OWB2.
7. Z. Zhang, R. Wang, and D. Xue, "Microfabrication by laser lithography combined with ion etching," in *Micro and Nano Fabrication Technology, Micro/Nano Technologies*, J. Yan, ed. (Springer, 2018), vol. 1.
8. X. Xiao, Q. Yu, Z. Zhu, K. Hu, and G. Chen, "Encoding method of CGH for highly accurate optical measurement based on non-maxima suppression," Chin. Opt. Lett. **15**, 111201 (2017).
9. P. Zhou and J. Burge, "Fabrication error analysis and experimental demonstration for computer-generated holograms," Appl. Opt. **46**, 657–663 (2007).
10. S. Peterhansel, C. Pruss, and W. Osten, "Phase errors in high line density CGH used for aspheric testing: beyond scalar approximation," Opt. Express **21**, 11638–11651 (2013).
11. L. Zheng, T. Hao, C. Guo, R. Wang, and Z. Zhang, "Phase analysis in computer generated hologram induced by direct laser writing systems with orthogonality error," Acta Optica Sinica **36**, 1012005 (2016).